Ocean Engineering 239 (2021) 109904

Contents lists available at ScienceDirect

Ocean Engineering

journal homepage: www.elsevier.com/locate/oceaneng

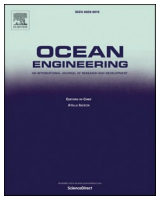

Method to assess the interplay of slope, relative water depth, wave steepness, and sea state persistence in the progression of damage to the rock layer over impermeable dikes

Miguel Á. Losada

Professor Emeritus, Andalusian Institute for Earth System Research (IISTA), University of Granada, Avda. Del Mediterráneo, s/n, 18006, Granada, Spain

ARTICLE INFO

Keywords:
Sloping coastal structures
Dimensional analysis
Damage evolution
Experimental design

ABSTRACT

The objective of this research was to develop a new methodology to assess the progression of damage to sloped coastal structures such as revetments, dikes, and mound breakwaters by applying dimensional analysis. The adequacy of the derived functional relationship was verified with the same experimental data (rock layer over impermeable dikes under irregular waves and four dike slopes) originally used to obtain the Van de Meer stability formula. The method addresses the epistemic uncertainty of the damage evolution model and its dependence on the experimental design and technique, the non-dimensional incident sea-state characteristics at the foot of the slope, relative water depth, relative wave height, wave steepness, sea-state persistence, and number of waves. It is specific to each dike slope. Specifically, the scarcity of experimental data in shallow water conditions are considered. Accordingly, the sigmoid function is proposed as an alternate model to quantify the progression. In the current state of knowledge, it is uncertain how the formulas based on lab-experiments perform for real-world design conditions. More research in the form of further test series is thus necessary to explore this new approach in greater depth.

1. Introduction

Forty per cent of the world's population lives near the coast and many of the world's major cities are directly located on the seashore. Spain alone, has a coastline of over 8000 km, roughly half of which is occupied by human activities. Global warming and one of its main effects, rising sea levels, call this territorial model into question. In the last several years, various alternatives for coastal protection, adaptation, and mitigation have been proposed. The challenge of protecting the coast from the effects of global warming necessarily involves quantifying the resilience of structures as well as their intrinsic and epistemic uncertainty. These new demands ask for new coastal and ocean engineering philosophy regarding the socioeconomic and environmental impact of human interventions (Baquerizo and Losada, 2008; Losada et al., 2009).

Revetments, dikes, and mound breakwaters are the most common type of sloped coastal structures because of their ability to break and/or dissipate wave energy. They can also be constructed with different materials, and their armor units can be of different shapes and sizes. Their design, construction and management are a major investment, which extends over successive phases throughout their life cycle since during their useful life, their state and conditions may change.

The effects of the intrinsic uncertainty (e.g., due to wave climate variability) were significant when computing the damage level in the middle of the 20th century. Nowadays, the quantification of epistemic uncertainty (Kroon et al., 2020), namely, the uncertainty introduced by the model of damage progression, S_d, of the principal failure modes, whether correlated or independent, is a major knowledge deficit in the optimization of coastal structures (Lira-Loarca et al., 2019; ROM 1.1, 2018). To effectively determine uncertainty and thus estimate the total investment cost (ROM 1.1, 2018), it is necessary to have predictive models of the hydrodynamic and structural behavior of the works over the useful life of the project.

In practical coastal engineering, the stability of the slope of rock-armored mound breakwaters is usually verified by applying laboratory-based empirical formulas. The earliest formula by Iribarren and Nogales (1949) and the reductionist/simplified version of Hudson (1959) were modified after the publication of Battjes (1974) on the surf similarity parameter.

Currently, most of the formulas used to verify the stability of the armor units of the main layer are formally like the Van der Meer (1988) formula, which is based on a significant number of experiments in a

E-mail address: mlosada@ugr.es.

https://doi.org/10.1016/j.oceaneng.2021.109904
Received 28 May 2021; Received in revised form 16 August 2021; Accepted 21 September 2021
Available online 25 September 2021

wave flume with different typologies. Van der Meer concluded that the stability of rubble mound revetments and breakwaters can be described by the following dimensionless variables, $\left(\frac{H_s}{D_{n50}\Delta_s}, \xi_m, cot\,\alpha, \frac{S_d}{\sqrt{N_w}}, P,\right)$ and proposed a formula for plunging waves and another for surging waves. In consonance with the state of the art, the formula did not include the relative water depth, h/L. $N_s = \frac{H_s}{D_{n50}\Delta_s}$ is the stability number (Hudson, 1959); α, is the slope angle; and ξ_m, o I_r, $I_r = \frac{\tan\alpha}{\sqrt{\frac{H_s}{L}}}$ is the Iribarren number (Iribarren and Nogales, 1949). D_{n50} is the nominal diameter of the rock layer, defined by $D_{n50} = (M_{50}/\rho_s)^{\frac{1}{3}}$, where M_{50} is the average stone mass, which is 50% of the value on the mass distribution curve; $\Delta_s = \rho_s/\rho_w - 1$, is the relative mass density; and ρ_s, ρ_w are the mass density of the rock and water, respectively.

According to Van der Meer (1987), $S_d = \frac{A_e}{D_{n50}^2}$ is the dimensionless damage, and A_e is the eroded cross-sectional area of the profile. A physical description of S_d is the number of cubic stones with a side of D_{n50}, eroded within a width of one D_{n50}. H_s and L are the incident significant wave height and wavelength, respectively, at the toe of the slope; N_w is the number of waves in the sea state; and P is a notional permeability parameter (Van der Meer 1988). It can be applied not only to calculate the stability number, N_s, based on the damage level, S_d, but also to calculate S_d based on N_s.

Despite its widespread use, the Van der Meer formula is subject to a permanent process of experimental revision. Most of these revisions are only refinements of the statistical wave descriptors used. Recently, Etemad-Shahidi et al. (2020) eliminated P and included a permeability coefficient C_p. Basically all of the revised formulas have the same formal structure and almost the same non-dimensional variables.

It is surprising that in the last 40 years few researchers have considered the effect of the relative water depth at the toe of the slope on the progression of damage under non-breaking conditions before the waves reached the structure. Melby and Hughes (2004) derived a stability formula based on the maximum wave momentum flux (Hughes 2004), and concluded that when the water depth was incorporated, a better description of stability (surging and plunging breaker types) was obtained.

Furthermore, as noted by Ahrens et al. (1993), and recovering the concerns of Hughes (2004), "there are few laboratory data for shallow water conditions of near depth-limited breaking relative to water depth at the structure toe". So, it can be concluded that there is no certainty about the performance of laboratory-based wave stability formulas for what may be the design condition for coastal protection under global warming.

The objective of this research was to develop a new methodology to assess the progression (or spatio-temporal evolution) of the damage to sloped coastal structures such as revetments, dikes, and mound breakwaters. This method was applied to a two-diameter-thick rock layer placed on an impermeable core and four dike slopes and verified with the same experimental data originally used to obtain the Van de Meer stability formula.

This method addresses some open questions related to the design of coastal protection with laboratory-based formulas that have an impact on uncertainty and total cost investment in regard to the following: (1) the role of the relative water depth h/L on the damage evolution, S_d and its interplay with the slope m and wave steepness H_I/L; (2) the dependence of the damage evolution, S_d, including the initiation of damage and destruction, on the experimental design and technique; (3) the performance of laboratory-based wave stability formulas for what may be the design condition.

The rest of this paper is organized as follows. In Section 2, the generalized Buckingham's π theorem (Sonin, 2001) is applied to obtain a function that relates the damage level and its spatiotemporal evolution to the characteristics of the wave train. Section 3 explores the form of the function and verifies it against the experimental data of Van der Meer (1988). Section 4 analyzes the interplay of the slope and the characteristics of the incident wave train on the progression of damage, including the generated value of the relative wave height, H_I/h. In section 5 the sources of epistemic uncertainty are discussed. Section 6 proposes, as an alternate model, the sigmoid function. This is followed in Section 7 by a brief discussion of the challenges of maritime engineering and physical experiments. The paper ends with a summary of the most important conclusions that can be derived from this research. The two appendixes show the fit and correlation coefficients, specific for each tested slope, 1:2, 1:3, 1:4 and 1:6, which were obtained for the linear relationship, eq. (10). Also included is the sigmoid function, eq. (12).

2. Reformulation of the spatiotemporal evolution of the damage to a sloping coastal structure

The structure used to test the methodology presented in this study is a sloping non-overtopped dike, composed of an impermeable core and a main layer of rock rubble. In this dike, α is the angle of the seaward slope. The independent variables governing the evolution of the main layer are the following (Losada and Giménez-Curto, 1979).

(a) environment: sea bottom slope β_b; depth at the toe of the slope, h; density ρ_w and dynamic viscosity of the water, μ; and gravity acceleration, g;
(b) incident waves: descriptors of the characteristic wave height and period, H_I and T_m; wavelength, L; energy spectrum, and incidence angle, θ;
(c) breakwater typology: main layer composed of rock rubble with a nominal diameter, D_{n50}; armor unit density, ρ_s; number of sublayers, n_c; sublayer thickness e; slope of the dike, $m = \tan\alpha$;
(d) time from the beginning of the experiment, t.

To form this complete set of independent variables, it was necessary to adopt certain simplifications, which did not alter the generality of the results obtained: horizontal bottom, $\beta_b = 0$; normal incidence, $\theta = 0$; and single-peak wave spectrum. Since the slope of the dike, m, is dimensionless, it is not included in the complete set of independent variables but is regarded as a previously specified geometric characteristic of the structure such as the type and shape of the armor unit.

The temporal evolution of the main armor layer is quantified by A_e, the eroded cross-sectional area of the profile. It is determined by the values of the following $n = 11$ independent quantities:

$$A_e = f(h,\ \rho_w, \mu,\ g, H_I,\ L,\ D_{n50}, \rho_s, e,\ t,\ T_m) \tag{1}$$

The persistence of the sea state can be unambiguously separated from the complete set of independent quantities to form the dimensionless variable $\left(\frac{t-t_0}{T_m}\right)$. Time t_0 is included to account for the state of the breakwater at instant t_0 and to satisfy the compatibility condition: "changes in the origin of times should not alter the accumulated damage value" (Castillo et al., 2012; Melby and Kobayashi, 1998, 1999). Then,

$$A_e = f_1(h,\ \rho_w, \mu,\ g, H_I,\ L,\ D_{n50}, \rho_s, e) * f_2\left(\frac{t-t_0}{T_m}\right) \tag{2}$$

The function f_1 depends on the rest of the complete set ($n = 9$). Among others, there are $n_F = 4$ variables that define the characteristics of the rubble mound layer and its thickness and the fluid dynamic viscosity $\{D_{n50}, \rho_s,\ \mu,\ e\}$, whose value remains constant throughout the experiment. Once a dimensionally independent subset is chosen, $k_F = 3$, $\{D_{n50}, \rho_s,\ \mu\}$, f_1 depends on a set of n-n_F+ $k_F = 8$ independent variables. Then, when a reduced set is selected from an independent subset of k variables, $\{\rho_w, g,\ L\}$, the non-dimensional eroded cross-sectional area of the profile should depend on a set of $N = (n$ - k) - (n_F - k_F) = 5 dimensionless variables and on the value of f_2 at the dimensionless time $\left(\frac{t-t_0}{T_m}\right)$,

$$S_d = \frac{A_e}{D_{n50}^2} = f_1\left(\frac{h}{L}, \frac{H_I}{L}, \frac{\rho_s}{\rho_w}, \frac{D_{n50}\sqrt{gD_{n50}}}{\frac{\mu_w}{\rho_w}}, \frac{e}{D_{n50}}\right) * f_2\left(\frac{t - t_0}{T_m}\right) \quad (3)$$

where S_d represents the dimensionless output, or the progression of the damage or cumulative damage at $\left(\frac{t-t_0}{T_m}\right)$, of the experiment. The third and fourth monomial in eq. (3) can be combined to define a single non-dimensional quantity, D_*,

$$D_* = \frac{D_{n50}\sqrt{g\Delta_s D_{n50}}}{\nu} \quad (4a)$$

$$\nu = \frac{\mu_w}{\rho_w} \quad (4b)$$

where, D_* is the particle parameter, first defined by Madsen and Grant (1976), who related it to the Shields parameter in conditions of incipient sediment transport. In the context of sloping breakwaters, it is a suitable armor unit parameter that can be used to analyze the scale effects (similar to a Reynolds number), and to compare the flow and stability of different types of units tested in the same conditions. Furthermore, by dimensionalizing the thickness of the main layer with the diameter of the armor unit, the functional relationship, eq (3) can be written as follows:

$$S_d = \frac{A_e}{D_{n50}^2} = f_1\left(\frac{h}{L}, \frac{H_I}{L}, D_*, e_*\right) * f_2\left(\frac{t - t_0}{T_m}\right) \quad (5)$$

As can be observed, the thickness of the main armor layer, e, is determined based on the nominal size of unit, D_{n50}, and on the shape factor of unit, K_p and the number of layers, n_c (Gómez-Martín and Medina, 2014),

$$e = n_c K_p D_{n50} \quad (6a)$$

$$e^* = \frac{e}{D_{n50}} = n_c K_p \quad (6b)$$

In the practical example (see Fig. 1), a sloping non-overtopped dike, composed of an impermeable core and a main layer of rock rubble, the nondimensional quantities e^*, D_*, Δ_s, and their corresponding dimensional quantities, n_c, K_p, D_{n50}, have a constant value in all the experiments. Under such conditions, the functional relationship between the dimensionless quantities, cumulative damage, incident wave characteristics, and persistence of the sea state is the following:

$$S_d = \frac{A_e}{D_{n50}^2} = f_1\left(\frac{h}{L}, \frac{H_I}{L}\right) * f_2\left(\frac{t - t_0}{T_m}\right) \quad (7)$$

Eq. (7) is the formal structure of the equation for the cumulative damage in a sea state and a storm (sequence of sea states). In addition, Bridgman's principle of absolute significance holds for the cumulative damage, S_d, (a physical quantity). It thus has a monomial formula (functional relationship) if it is in the form of a specific power-law. Díaz-Carrasco et al. (2020), Clavero et al. (2020) and Moragues and Losada (2021) showed that the product of the relative water depth and wave steepness at the toe of the dike, $\chi = \frac{h}{L}\frac{H_I}{L}$, is an alternative similarity parameter to the Iribarren number and can be used to quantify the wave breaker type, flow characteristics, and wave energy transformation on the slope. For this reason, a monomial formula with the same power-law form obtained was chosen to describe the cumulative damage of the rock layer over impermeable dikes,

$$S_d = \frac{A_e}{D_{n50}^2} = f_1(\chi) * f_2\left(\frac{t - t_0}{T_m}\right) \quad (8)$$

This signifies that the results are dimensionally homogeneous and intuitively interpretable. The $\pi-$theorem does not provide the form of the functional relationship. This form can only be obtained by physical or numerical experimentation or by theoretically solving the problem (Sonin, 2001). In this study the choice of functions $f_{1,2}$ is based on data (Shen et al., 2014), which depend on the experimental design and technique. More specifically, these are the following: (i) slope of the dike; (ii) sample space defining sequences of subsequent sea state pairs $(h/L, H_I/L)$ and their persistence or number of waves, N_w; and (iii) the criteria determining the sounding strategy of the cumulative damage once the test is finished, and the section is rebuilt. Accordingly, $f_{1,2}$ were then selected to model Van der Meer's experimental output.

2.1. Graphical representation of the experimental design and sample space

The sample space (Fig. 2) is the geometric locus of the experimental points defined by their coordinates, wave steepness and relative water depth. From a geometric perspective, the limit values of h/L and HI/L in the wave flume are determined by the water depth at the toe of the dike, h, and slope, m, and, if applicable, the characteristics of the mantle and core, which are the sides of the quadrilateral.

The log transformation of the relative water depth, h/L, and wave steepness, H_I/L, was applied. For the sake of completeness, the figure includes the maximum wave steepness of a regular progressive wave train propagating in a constant water depth as calculated with Miche's (1944) equation.

Each line $\chi = (H_I/L)(h/L)$ is the geometric location of wave trains of the same breaker type (Moragues and Losada, 2021). Their location depends on and is specific to the slope gradient and the characteristics of the dike. Moreover, each line $\gamma = (H_I/L)/(h/L) = H_I/h$ is the geometric location of wave trains with the same relative wave height at the toe of the slope. Their location depends on the characteristics of the wave flume and its generation system.

The sample space helps to identify and select the values of the main parameters, $(h/L, H_I/L)$ as a function of the slope m, generation system, breaker type (χ), and the relative wave height (γ). In contrast to Battjes

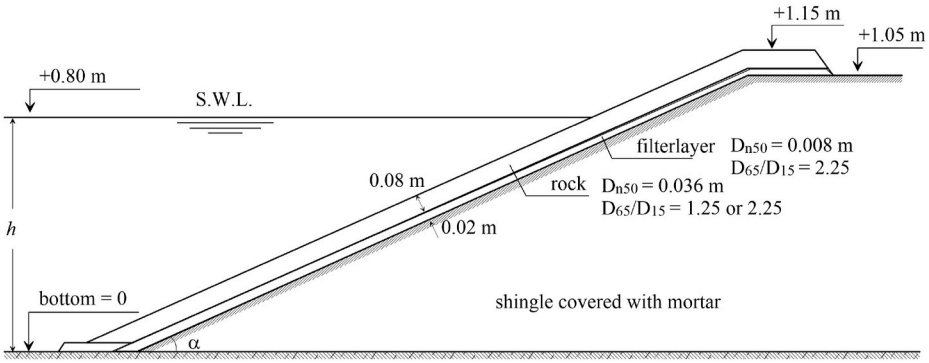

Fig. 1. Tested structure with a double armor layer and an impermeable core (Van der Meer, 1988).

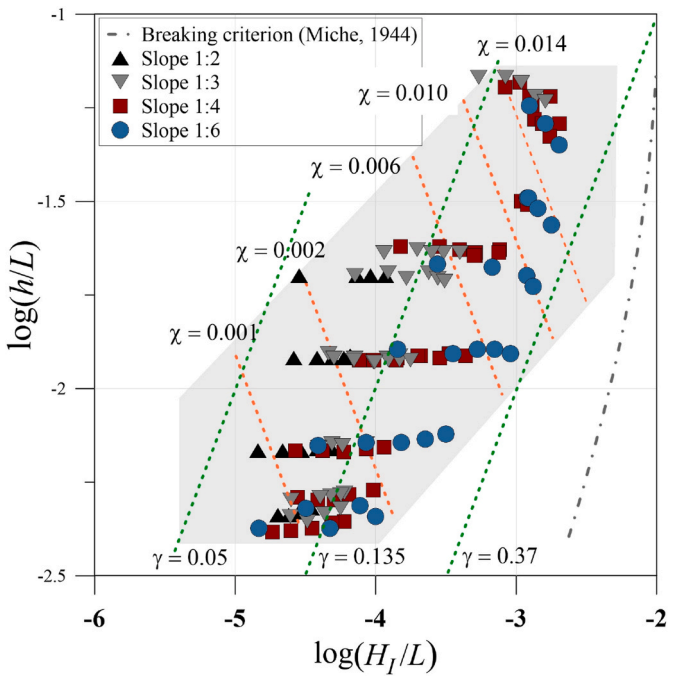

Fig. 2. Sample space of Van der Meers, (1988) experiments for a dike with a double armor layer and an impermeable core. Four slopes were tested. The red straight dashed lines represent the constant value of $\chi = \frac{h}{L}\frac{H_I}{L}$. The green straight dashed lines represent the constant value of $\gamma = \frac{H_I}{h}$. Wave-breaking criterion by Miche (1944) is also shown. (For interpretation of the references to colour in this figure legend, the reader is referred to the Web version of this article.)

(1974), the dependence of the relative water depth cannot be ignored since for each value of the depth and slope, different sequences of breaker types and relative wave height are obtained. In addition, they depend specifically, among others, on the slope *m*. As can be observed, the sample space is a continuum, and real values of h/L and H_I/L depend on the generation system as well as the experimental design and technique.

3. Fitting the function to the experimental data of Van der Meer (1988)

This section analyzes the damage observed during wave flume experiments on the rock layer over impermeable dikes by Van der Meer (1988). In the experimental set, the dike was constructed using the same rock type, nominal diameter, and relative density, and $n_c = 2$. Since a water depth of $h = 0.80$ *m* was applied in all the tests, h, D_*, and e_* remained constant. Four slopes were tested (1:2, 1:3, 1:4, and 1:6), which meant that there were four different datasets to fit to the corresponding function. Fig. 2 shows Van der Meer's (1988) sample space for the four slopes. The majority of the experimental points are located inside a hexagon with parallel sides, two by two. The red straight dashed lines represent the constant value of $\chi = \frac{h}{L}\frac{H_I}{L}$. The green straight dashed lines represent the constant value of $\gamma = \frac{H_I}{h}$.

Van der Meer (1988) carried out the experiments (experimental technique) in Test Series (TS). Generally, a TS consisted of five complete tests (CTs) with the same average wave period, (constant h/L) but with increasing incident significant wave heights, H_I. The output of a test series (TS) generally consisted of two sets of data ($N_w = 1000$ and 3000) of five pairs of values of S_d, (corresponding to a given h/L and five increasing values of H_I/L). It consisted of a pre-test sounding, a test of 1000 waves, an intermediate sounding, a test of 2000 more waves, and a final sounding. After each complete test the armor layer was removed and rebuilt. Because of the experimental technique for each CT, $t_0 = 0$, and $t/T_m = N_w$ were the average number of waves in the test, and $f_2(N_w)$.

Therefore, based on the method of dimensional analysis (DA), for each slope *m*, and for number of waves, N_w, there is a functional relationship between the output, S_d, and the alternate slope similarity parameter,

$$S_d = \frac{A_e}{D_{n50}^2} = f_1(\chi) \tag{9}$$

When $S_d \sim \chi$ is selected and the log is taken on both sides, eq. (9) produces a 'linear model',

$$log(S_d) = A_m log(\chi) + B_m \quad \chi_{min} \le \chi \le \chi_{max} \tag{10}$$

A_m and B_m are the fit coefficients of the straight line which are specific to each of the slopes (1:2, 1:3, 1:4, and 1:6) and number of waves, $N_w = 1000$ and 3000. Table 1 shows the fit parameters and correlation coefficients for slope 1:3, $N_w = 1000$ and 3000 waves, and relative water depth, h/L. R^2 is the linear regression coefficient. In Appendix Ia, Table A-I gives the parameters of the straight line for the other three slopes 1:2, 1:4, and 1:6. Van der Meer (1988) noticed the existence of a linear relation for $N_w = 0$–1000 waves. By using a log-transform of the sample space, it is possible to anticipate the experimental results of each CT (wave steepness) of a TS (relative depth). As can be observed, χ_{min} and χ_{max} in eq. (10) define the interval of application of the equation (i.e., the experimental interval).

Fig. 3 shows the experimental values and the best-fit lines of log (S_d), based on log (χ), for a slope of 1:3 and seven relative water depths, after being impinged by $N_w = 1000$ and 3000 waves. For each relative depth, h/L, log (S_d), and log (χ) have an approximately linear relation. The data corresponding to low values of h/L (shallow water) are located to the left of the graph, where the most probable breaker types are surging or collapsing breakers. The data for intermediate and deep water are located to the right of the graph, where the most probable breaker types are collapsing or plunging breakers. In all cases, the damage level becomes greater as $\frac{H_I}{L}$ increases, in other words, as the wave height increases (and N_s).

The fit lines of the two sets of number of waves slightly converge as the damage level decreases (start of damage) and they slightly diverge as the damage level increases (destruction). As can be observed, practically all of the five tests with $N_w = 1000$ end with a damage level lower than that observed with $N_w = 3000$. Limits χ_{min} and χ_{max} in eq. (10) correspond to the start of damage $S_{d,0}$ and a representative value of destruction, $S_{d,max}$, respectively, as discussed in section 5. Indeed, Van der Meer (1988, Table, 3.2) indicates that $S_{d,0} = 2$, log (2) ≈ 0.70, and $S_{d,max} = 12$, log (12) ≈ 2.5 should be considered for start of damage and destruction, respectively when a static stable structure of rock is designed with slope 1:3.

Table 1
Parameters of the straight line, eq. (10), for slope m = 1:3, N_w = 1000 and 3000 waves, and relative water depth h/L. R^2 is the linear regression coefficient.

Slope 1:3						
	S_d $Nw = 1000$			S_d $Nw = 3000$		
h/L	A_m	B_m	R^2	A_m	B_m	R^2
0.30949	3.4497	15.930	0.98554	4.4798	20.698	0.94498
0.29342	4.1001	18.853	1	5.2731	24.100	1
0.19491	4.1007	23.166	0.98125	4.2227	24.296	0.99445
0.18397	4.9895	28.353	0.88521	5.2536	30.467	0.99941
0.18173	4.4276	25.518	0.95502	4.9084	28.536	0.97837
0.14652	5.0081	30.973	0.97488	4.4410	28.227	0.92096
0.11634	8.4794	55.485	0.98106	8.9923	59.262	0.96935
0.10156	5.8899	40.460	0.97210	5.6138	39.109	0.94567
0.09656	3.8557	27.696	0.44339	4.5784	33.080	0.49069

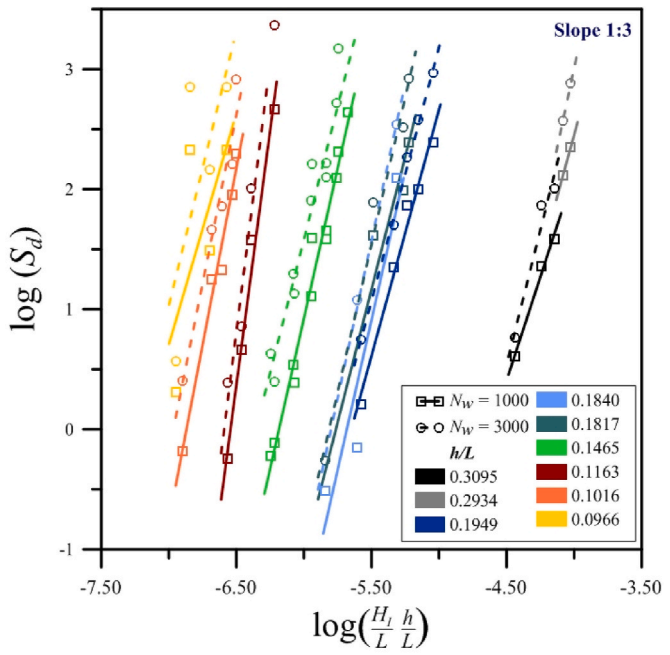

Fig. 3. Fit of eq. (11) to experimental data for a slope of 1:3 and different values of the relative water depth after Nw = 1000 and 3000 waves. Each test series (TS) was performed with a constant value of the relative depth, h/L and consisted of a variable number of complete tests (CT). Each CT was performed with a constant value of H_I/L, which was increased in the following CT.

4. The interplay of the non-dimensional independent quantities in the evolution of damage

For a given number of waves, the interplay of the three quantities, h/L and H_I/L, and slope, m, is most usefully and accurately represented by graphical representations in a 2D system in terms of pairs of values, while the other quantity remains constant. Accordingly, there are three possibilities: (i) to combine values of h/L, and H_I/L while m remains constant (Fig. 3); (ii) to combine values of m and H_I/L while h/L remains constant (Fig. 4); or (iii) to combine values of m and h/L while H_I/L remains constant.

Fig. 4 shows the log-transform of the cumulative damage, S_d, against the log-transform of the slope m = 1:2, 1:3, 1:4, 1:6, for three relative water depths, (a) $h/L \approx 0.1863$, (b) $h/L \approx 0.1496$, and (c) $h/L \approx 0.0970$, several values of $\chi = \frac{h}{L}\frac{H_I}{L}$, and $N_w = 1000$ waves. The values of $log\ (S_d)$ were calculated by applying the linear relationship, eq. (12). Its coefficients, A_m, B_m, depend on the relative water depth and the slope, and are given in Table 1 for slope m = 1:3, as well as in Appendix I (see Table I-A for the other three tested slopes m = 1:2, 1:4, 1:6).

For the set of milder slopes, (1:6 and 1:4), as the slope steepens, the damage grows with increasing wave steepness and decreasing water depths, except for large values of h/L and small values of H_I/L. For the set steep slopes (1:3 and 1:2), the growth rate of the damage depends on the relative values of slope, m, h/L, and H_I/L. However, the highest damage levels are produced with small values of h/L, large values of wave steepness, and slope m = 1:3. For $h/L = 0.1496$ the worst damage always occurs with m = 1:2. For $h/L = 0.097$ the worst damage depends on the wave steepness.

Except for low wave steepness, the damage generally increases as the slope and wave steepness increases. The growth rate depends on the relative water depth. For the same wave steepness, the damage is greater as h/L decreases. Although there is no information pertaining to m = 2:3 and h/L <0.095, based on other experimental data (Iribarren, 1965; Losada and Giménez-Curto, 1979; Losada et al., 1986), it can be generally assumed that for a given N_w, the growth rate of the cumulative damage is not a monotonic function of the slope, and depends on the relative values of h/L and H_I/L. The effects are concomitant as described by the alternate similarity parameter, $\chi = (h/L)(H_I/L)$ as shown in the following sections. The singular behavior of the slope is relevant to the analysis of the performance of sloped coastal structures under oblique wave attack (Losada and Giménez-Curto, 1982).

As can be observed, the persistence of the sea states is different although the average number of waves is the same, $t = N_w{*}T_m$. The sea states with a larger average wave period are of longer duration. Losada and Giménez-Curto (1981) obtained the relation between the failure probability when the persistence of the sea state is t hours and the failure probability when the persistence of the sea state is 1 h. These results highlight the importance of sea state persistence in relation to failure probability.

4.1. Interplay of h/L and H_I/L for a fixed damage level (Nw = 1000 and slope 1:3)

Fig. 5 shows the sample space (log-transform of H_I/L and h/L) of Van der Meer's (1988) experiments for a dike with a double armor layer and an impermeable core and slope, m = 1:3. The points identify the pairs of values of wave steepness and relative water depth for fixed damage levels S_d = 1, 2.7, 7.4, 20.1, 24, after impinging N_w = 1000 waves. Fit curves are drawn for each set of five values. The values of S_d are calculated by applying eq. (10). Coefficients A_m, B_m are given in Table 1 (and also in Table I-A of Appendix I for slopes 1:2, 1:4, and 1:6). For a given value of S_d, and once chosen the slope m, water depth, h, and average wave period T_m, then eq. (11) can be used to obtain the log-transform value of the wave steepness, $log\ (H_I/L)$, (x-axis, Fig. 5).

The colour bands in Fig. 5 are separated by lines of constant χ and determine the transition of the breaker types on the slope. For slope 1:3, an estimate of the domains where each breaker type prevails is the following: surging, $\chi \leq 0.0008$; weak bore, $0.0008 < \chi \leq 0.0012$; strong bore, $0.0012 < \chi \leq 0.002$, and strong plunging $0.002 < \chi \leq 0.01$. Their position and value are approximate and are based on Galvin's classification as extended by Moragues and Losada (2021) and on Van der Meer (1988).

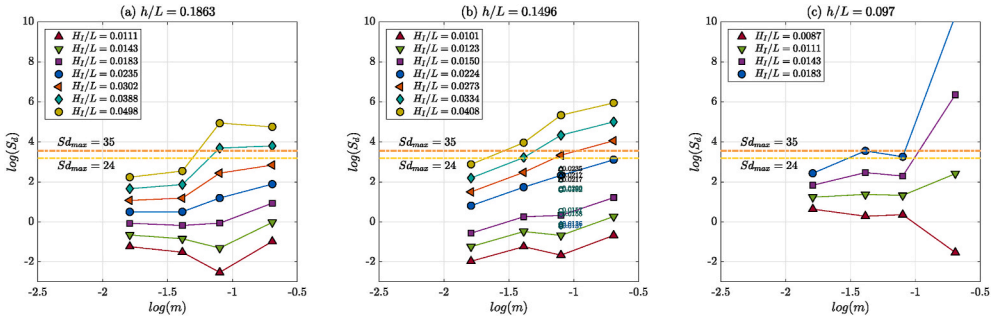

Fig. 4. Variation of the cumulative damage with the slope of the dike for N_w = 1000 waves. The three subfigures correspond to three relative water depths: (a) h/L ≈ 0.1863; (b) h/L ≈ 0.1496 and (c) h/L ≈ 0.0970. The sequence of increasing wave steepness is different for each relative water depth. The numbers in Fig. 4(b) are measured values of S_d in a slope 1:3, h/L ≈ 0.1496 and N_w = 1000 by Van der Meer (1988). The color matches the value of the constant wave steepness line. (For interpretation of the references to colour in this figure legend, the reader is referred to the Web version of this article.)

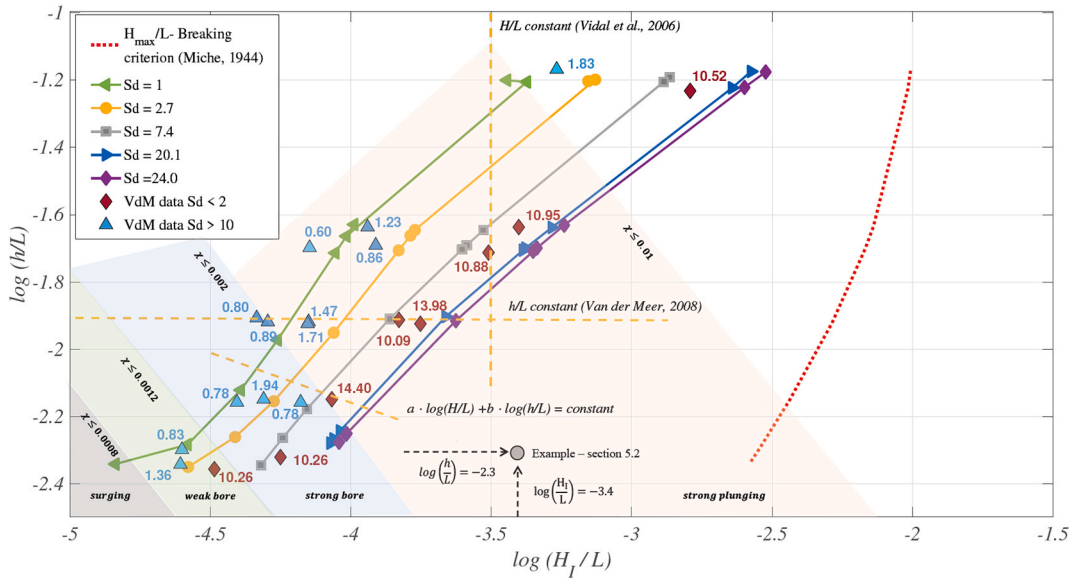

Fig. 5. Concomitant values of h/L and H_I/L which cause the same damage level, S_d, in a dike with a double armor layer and an impermeable core and slope 1:3 after impinging Nw = 1000 waves. Each curve corresponds to a fixed damage level in the interval $S_{d,0} \leq S_d \leq S_{d,max}$. The numbers are measured values of S_d by Van der Meer (1988). Estimated types of wave breakers and the input data for the example, section 5.2, are shown.

4.2. The limited generated relative wave height, H_I/h

It should be highlighted that the form of the cumulative damage curves changes significantly for relative shallow water depth, (Figs. 5 and 6). Unfortunately, Van der Meer tested all the slopes with h/L>0.090 and $\gamma = \frac{H_I}{h}$ in the interval [0.05 < H_I/h < 0.37] (Fig. 2). However, for the shallow-water test series, $h/L \approx 0.095$, the interval was even narrower, [0.10 < H_I/h < 0.20] (Fig. 5).

This is a standard limitation of the wave flumes that needs to be considered and standardized. So, according to Hughes (2004), it is uncertain how the derived formulas based on lab-experiments perform for what may be the design conditions.

4.3. Potential design curves in function of the stability number and h/L for selected damage levels

Fig. 6 shows potential design curves ($N_s = \frac{H_I}{\Delta_s D_{n50}}$ versus the log-transform of h/L) derived from Van der Meers, (1988) experiments for a dike with a double armor layer and an impermeable core and slope, m = 1:3. The curves provide the value of the stability number for fixed values of the damage level S_d = 1.0, 2.7, 7.4, 20.1, 24.0, after impinging N_w = 1000 waves. The input data are the incident significant wave height, H_I, and mean wave period, T_m, the water depth at the toe of the structure, the relative density of the rock, and the damage level, S_d. For a specific value of h/L (water depth and mean wave period), the curves provide the values of N_s (and thus of H_s) to determine the evolution of the damage level from S_d = 1.0, up to a value of 24.0, after impinging N_w = 1000 waves (see Fig. 5). It should be underlined that the calculated incident significant wave heights are linked to the selected mean wave period T_m, in other words, the chosen value of h/L. Therefore, the potential design curves provide a simple method of assessing the dependence of the damage level, S_d, on the wave period. The stretches of each dashed line have different slope because they were obtained from experimental data for discrete h/L values.

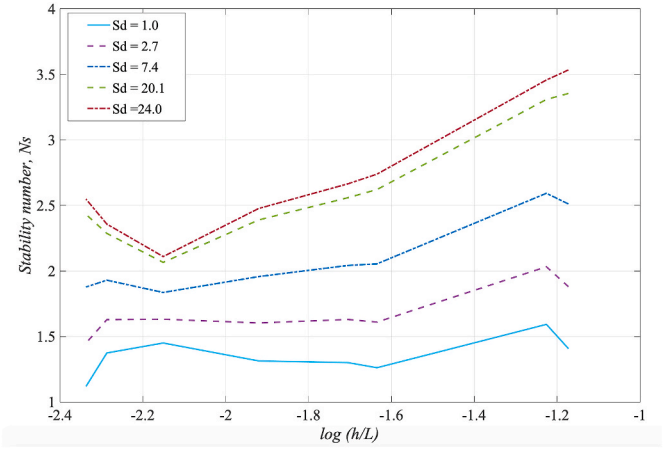

Fig. 6. Values of the stability number, Ns, in function of the relative water depth which cause the same damage level, S_d, in a dike with a double armor layer and an impermeable core and slope 1:3 after impinging Nw = 1000 waves. Each curve corresponds to a fixed damage level in the interval $S_{d,0} \leq S_d \leq S_{d,max}$, as shown in Fig. 5.

4.4. Dependence of damage evolution on experimental design and technique

The experimental design and technique specify the way the Test Series are carried out: (a) the relationship between h/L and H_I/L; (b) number of waves; and (c) when the section is rebuilt. This relationship is generally one of the following (see Fig. 5): constant h/L (horizontal trend), constant H_I/L or I_r (vertical trend) and a linear relationship between log(h/L) and log (H_I/L) (oblique trend), as represented in the equation,

$$Y = aX + b \tag{11}$$

where, Y = log (h/L), X = log (H_I/L), and a and b are the slope and the independent parameter of the straight line.

As reflected in Fig. 5, the Test Series (TS) of the Van der Meer (1988) experiments follow lines of constant h/L, or to be more precise, of constant period. In addition, the damage evolution in each Complete Test (CT) was observed after impinging N_w = 1000 and 2000 more waves with constant H_I/L. Once the CT finished, the section was reconstructed.

Vidal et al. (2006) studied a breakwater with slope 1:2 and performed TS, where the value of the Iribarren number, I_r (i.e., wave

steepness) remained constant, and $N_w = 500$ for regular waves and $N_w = 1000$ for irregular waves. Then, without rebuilding the section, they gradually increased the significant wave height and wave period, while I_r remained constant (by increasing both H_I and T and maintaining the water depth constant). As a result, each subsequent TS had a lower relative water depth. Fig. 7a and b shows the damage evolution compared to log ($h/L^*H_I/L$) under irregular and regular waves, respectively. As can be observed, the damage grows as log (χ) decreases, in other words, with a constant wave steepness (larger wave height and wave period) and a shallow water depth (constant water depth and larger wave period).

In the context of a different experimental design and technique, the damage evolution curves of the same breakwater typology could be different. Van der Meer rebuilt the section after CT and $N_w = 3000$ waves with h/L constant. Vidal et al. (2006) rebuilt the section after reaching the destruction of the slope with (H_I/L constant). The link between experimental design and technique, data analysis, and the evolution of damage depends on the interplay of the slope, wave steepness, relative water depth and the persistence of the sea state. Consequently, the datasets of Van der Meer (1988) and of Vidal et al. (2006) are not homogeneous.

5. Sources of epistemic uncertainty of the lab-based stability formulas

The prediction of the damage evolution of sloped structures for coastal and harbor protection is at the core of their design and estimate of their total investment cost (ROM 1.1, 2018). These predictions and their impact on the surrounding coastline are influenced by many uncertainties. A distinction is generally made between intrinsic and epistemic uncertainty (Van Gelder, 2000). Epistemic uncertainty is related to current knowledge regarding processes, models, observations, and methods. This section examines the epistemic uncertainty in the lab-based stability formulas developed following the Van der Meer (1988) methodology. The sources of uncertainty considered are the following: (1) exclusion of the non-dimensional parameter relative water depth, h/L; (2) scarcity of experimental data due to the limitation of the relative wave height; and (3) mixing of non-homogeneous lab data to develop a new formula.

5.1. Exclusion of the relative water depth h/L

The first and most important step in dimensional analysis is to identify a complete set of independent quantities that determine the value of the dependent variable (damage, S_d). However, if, the analysis is based on a set that omits even one independent quantity that affects the value, the dimensional analysis will give erroneous results (Sonin, 2001).

Van der Meer (1988) based the selection of non-dimensional variables on empirical grounds and other formulas rather than on dimensional analysis. The set of variables selected by Van der Meer (1988), namely, the slope, Iribarren number, I_r, stability number, N_s, number of waves, N_w, and the notional permeability parameter, P, cannot be deduced with dimensional analysis. At that time, following Battjes (1974), the formula did not include the relative water depth.

Fig. 8 shows the damage level measured in the laboratory as compared to the damage level calculated with the formula (Eqs. 3.23, 3.24, and 3.25 in Van der Meer (1988), with $N_w = 3000$ waves, of the rock layer over an impermeable slope 1:3. The relative water depth values are identified. The formula does not account for the scatter that can be observed in the results, which increases as the damage level grows. This scatter depends on the interplay of relative water depth, the wave steepness and slope, and on the small values of the relative water depth.

In Van der Meer's experiments, the majority of the trials pertain to Iribarren damage. There are only a few data regarding the start of damage and destruction. Table, 3.2 of Van der Meer (1988) shows that it would be wise to consider $S_{d,0} = 2$ and $S_{d,max} = 12$ in the design of a statically stable rock structure with a slope 1:3. This information makes it possible to design and calculate a rock layer over an impermeable dike with a slope, m, so that it can withstand a given sea state and undergo damage within the interval $S_{d,0} < S_d < S_{d,max}$.

5.2. Scarcity of experimental data in shallow water with large values of H_I/h and possible consequences

This prudent interval of application is further motivated because of the experimental limitations of the wave flumes to generate non-breaking shallow-water wave trains arriving at the toe of the slope with $H_I/h > 0.14$. The following example should clarify the problem.

The objective was to calculate the damage to an impermeable rock slope, $D_{n50} = 0.6$ m, $\Delta_s = 1.63$, with a slope angle 1:3, and water depth at the toe $h = 6$ m for a sea state with incident significant wave height $H_I = 2$ m, and wave period $T_m = 8.3$ s, at the toe of the slope and $N_w = 1000$ waves impinging on the structure. The dimensionless parameters of the design are, $h/L = 0.1001$; $H_I/L = 0.0333$; $\chi = 0.0033$; and $\gamma = 0.3333$. As can be observed, [Fig. 2, log (h/L) $= -2.3$ and log ($H_I/L = -3.4$], this sea state was not tested by Van der Meer (1988).

The available experimental data are in the interval shown in Fig. 3 and eq. (10), ($0.0010 \leq \chi \leq 0.0015$). Applying eq. (10) for (χ_{inf}, χ_{sup}) =

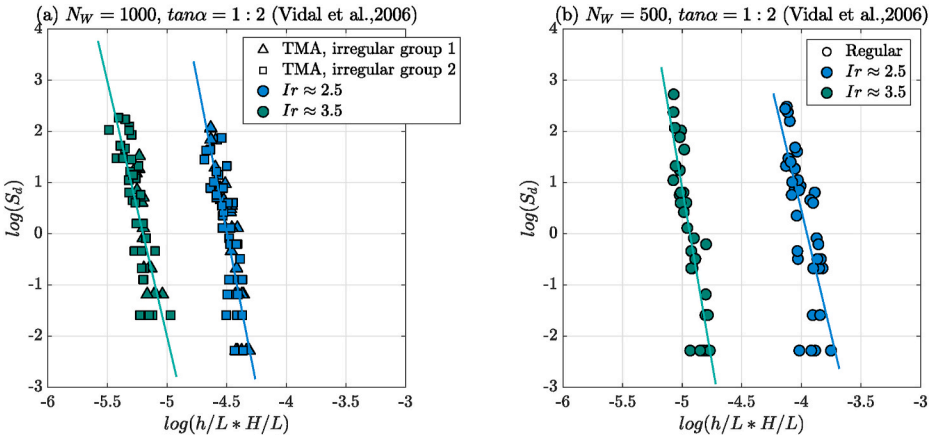

Fig. 7. Evolution of cumulative damage S_d of the rock armor layer of a permeable breakwater observed by Vidal et al., (2006), (a) under irregular wave trains (TMA spectrum) and $N_w = 1000$ waves per CT, and (b) under regular wave trains and $N_w = 500$ waves per CT. The section was rebuilt after reaching the level of destruction.

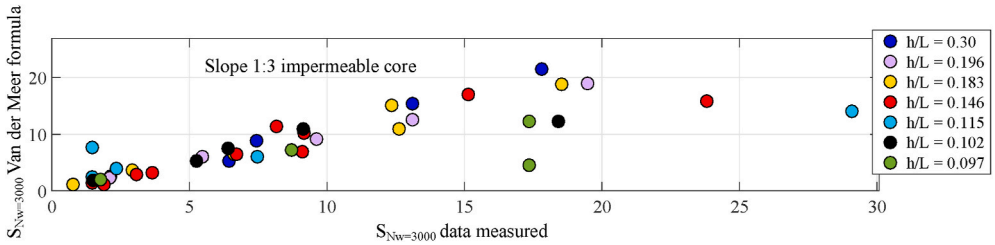

Fig. 8. Damage levels measured in the laboratory as compared to the damage level calculated with the formula (Eqs. 3.23, 3.24 and 3.25) of Van der Meer (1988), with $N_w = 3000$ waves.

(0.0010, 0.0016); (H_{inf}, H_{sup}) = (0.60, 0.96); ($N_{s,inf}$, $N_{s,sup}$) = (0.62, 0.98); the following damage interval ($S_{d,inf}$, $S_{d,sup}$) = (1.4, 13.3) is obtained. These values are very close to the experimental values. The expected wave breaker types are weak and strong bore. Mantle destruction, $S_{d,max} \approx 24$, would have occurred with $\chi \approx 0.0018$ and $\gamma \approx 0.18$, ($H_{I,d} = 1.08$; $N_{s,d} = 1.10$), under strong bore wave breakers. The example $h/L = 0.1001$, $\chi = 0.0033$, and $\gamma = 0.3333$, is evidently outside the application range of the model and in the domain of strong plunging breakers. Under such conditions, eq. (10) is not valid and without experimental information the prediction of the damage level would be very uncertain.

On the other hand, according to Van der Meer's (1987) formula, his eq. (11), for $m = 1{:}3$, $\xi_z = 2.44$ (his eq. (4) and plunging breakers and $a = 4.1$), and $N_s = 2.08$, $N_w = 1000$, then $S_d \approx 10 \neq 24$, (see his Fig. 3). The formula is unable to accurately predict the damage to the structure.

5.3. Mixing data from different experimental designs and techniques to develop a new formula

Fig. 9 shows the same dataset for the damage level measured in the laboratory, as compared to the damage level calculated with the revised formula of Etemad-Shahidi et al. (2020), with $N_w = 3000$ waves impinging on the rock layer of an impermeable slope 1:3. The new formula is based on a large number of non-homogeneous experimental datasets, (among others, data from Van der Meer, 1988 and Vidal et al., 2006). The scatter is much larger than the original Van der Meer formula.

6. An alternate prediction method: the sigmoid function

Following Iribarren (1965), Losada and Giménez-Curto (1979) and Vidal et al. (2006), the damage level can be organized in three regions: (i) start of damage $S_{d,0}$; (ii) developing damage, or Iribarren damage, S_d; (iii) destruction, $S_{d,max}$. As representative values of the two regions, start of damage, $S_{d,0}$, and destruction, $S_{d,max}$, comply with the following inequality, $0 < S_{d,0} < S_d < S_{d,max}$. (See Herrera et al., 2017 for further details).

Therefore, start of damage, $S_{d,0}$, and destruction, $S_{d,max}$, are specific to the response of a certain dike/breakwater typology and should depend on the nature of the dike (ROM 0.0, 2002). Furthermore, they should play an important role in the optimization of dike design and total cost during the dike's useful life (PIANC, 2016; ROM 1.1, 2018). There are two reasons for this. The first reason is that the dike's design should consider the shape of the transitions between the three regions and the subsequent influence of the change of wave breaker type. The second reason is that the scope of the dike/breakwater design should be widened so that it includes the role that such transitions play in the organization of the total project in its useful life. This pertains to the processes, resources, repair strategies, elaboration of decision trees, and finally the analysis of the profitability and risk level of the investment. This knowledge is essential to optimize (economically and environmentally) the design of the coastal structure in view of the predicted sea level rise in the present and in future years.

Accordingly, this study proposes, as a first stage, the sigmoid function, which incorporates representative values of the start of damage and destruction regions, ($S_{d,0}$, $S_{d,max}$). The application of the sigmoid function to model the evolution of damage in a slope has a theoretical justification (Churchill and Usagi, 1972). This function has often been used in other engineering fields and has been successfully applied to quantify the hydrodynamic performance of sloped impermeable structures and mound breakwaters (Vílchez et al., 2016; Díaz-Carrasco et al., 2020; Moragues et al., 2020). It should be useful in their experimental design and also improve the experimental technique and tools used.

In this research, the function was slightly modified to model $S_d/S_{d,max}$, the ratio between the observed damage and the representative damage of the destruction region,

$$\frac{S_d}{S_{d,max}} = \frac{1}{\left[1 + \left(\frac{\log(\chi)}{a_\chi}\right)^{\gamma_\chi}\right]} \quad 0 \leq \frac{S_{d,0}}{S_{d,max}} \leq \frac{S_d}{S_{d,max}} \leq 1 \tag{12}$$

where γ_χ is a blending coefficient that describes a uniform transition between the limit values of the maximum and minimum level of damage ($S_{d,0}$, $S_{d,max}$); and a_χ is the inflection point of the sigmoid curve, which is specific to each slope angle, m, and relative water depth, h/L. Consequently, the sigmoid curve determines the interval of log (χ) (i.e: H_I/L) in which the damage level evolves from the start of damage, $S_{d,0}$ to destruction $S_{d,max}$. The parameters of the sigmoid in eq. (12), (γ_χ, a_χ),for slope 1:3 with 95% confidence bounds for $N_w = 1000$ and 3000 waves are given in Appendix Ib.

Start of damage, $S_{d,0}$, is characterized by the random behavior of its values between zero damage and an upper bound. On average, $S_{d,0}$

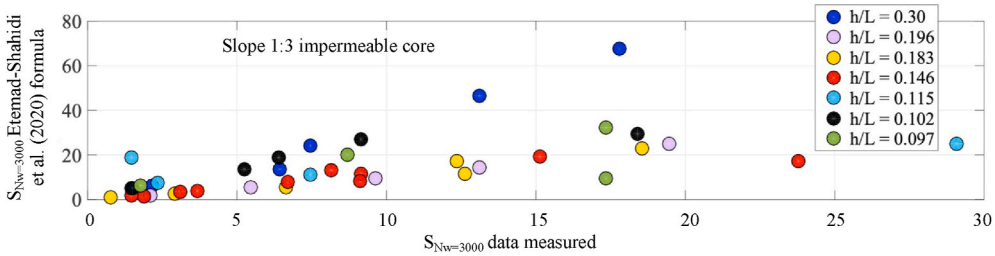

Fig. 9. Damage levels measured in the laboratory by Van der Meer (1988) as compared to the damage level calculated with the formula (Eqs. 17a, 17b) of Etemad-Shahidi et al. (2020) with $N_w = 3000$ waves.

slowly evolves with log (χ) in the start-of-damage region until a threshold is reached after which the evolution rapidly increases for moderate increases of log (χ), (i.e., increases of H_I or N_s). The threshold value for each slope more or less corresponds to the value given in Table, 3.2 in Van der Meer (1988). The advantage of this definition of damage is that it does not depend on the length of the slope (Van der Meer, 1987). It is then shown that the wave steepness values, H_I/L (H_I or N_s) that are required to reach this threshold also depend on the relative water depth, h/L.

A representative value of the destruction region depends on the availability of materials to develop an S-profile and on the type of wave breaking. This influences the evolution of damage in the destruction region as described and analyzed by Iribarren (1965), Ahrens (1989), Torum (1998), Losada et al. (1986), Melby and Kobayashi (1999), Kobayashi et al. (2010) and Kobayashi et al. (2013).

Fig. 10 represents the quotient $S_d/S_{d,max}$, which varies in the interval [0,1], depending on log (χ): (a) $N_w = 1000$ waves; (b) $N_w = 3000$ waves, and slope 1:3. $S_d/S_{d,max}$ represents the damage rate that is exceeded when log (χ) is greater than a certain value. In addition, this quotient quantifies the proportion of the number of stones displaced in relation to those displaced in the destruction of the breakwater. Once the relative depth is selected, the graph could represent the proportion of the destruction of the main layer, depending on H_I or the stability number.

The sigmoid function replicates the output results of each TS (h/L constant), measured in a slope m impinged by an average number of waves, N_w. However, to capture the damage evolution of both the upper and lower tails of the sigmoid function based on lab-experiments, the experimental design and technique must be significantly improved. This is a major challenge for maritime engineering.

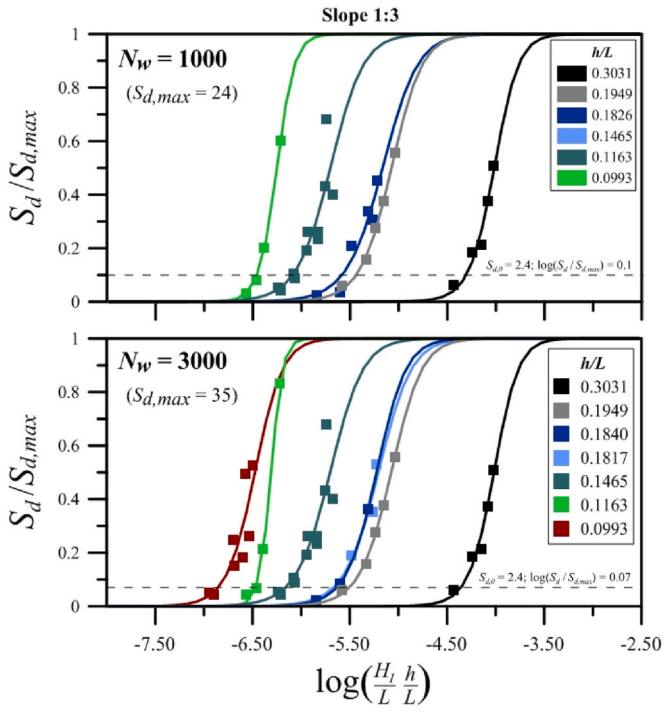

Fig. 10. Damage rate $S_d/S_{d,max}$ depending on log(χ). A sigmoid curve is fitted for each relative water depth to the experimental data for slope of 1:3. (a) $S_{d,0} \geq 0$ and $S_{d,max} = 24$ and $N_w = 1000$. (b) $S_{d,0} \geq 0$ and $S_{d,max} = 35$ and $N_w = 3000$. $\chi = \frac{h}{L}\frac{H_I}{L}$. $S_{d,0} = 2.0$ and $S_{d,max} = 12.0$ are the recommended values when a statically stable structure of rock with a slope 1:3 is designed (Van der Meer 1988).

7. The challenge of maritime engineering

As previously mentioned, the objective of this paper was to stimulate innovative research to improve the design tools based on knowledge of the performance of coastal structures under wind-wave and long-wave actions. The overall performance of revetments, dikes, and mound breakwaters depends on the kinematic and dynamic regimes as well as on the incident wave transformation when the wave train interacts with the structure. Its quantification should thus take into account the following three laws: (1) the energy conservation law used to estimate the energy transformation in the wave-structure interaction; (2) the mass conservation law, applicable to the calculation of run-up, run-down, and overtopping; and (3) the momentum conservation law, used to calculate the forces and momentums on the armor units of the maritime structure (ROM 0.0, 2002; ROM 1.1, 2018).

In his seminal paper, Battjes (1974) proposed using the Iribarren number to characterize a number of surf variables, namely breaker type, wave energy transformation, and flow characteristics. Ahrens and McCartney (1975) and Bruun and Günbak (1977) added the K_D factor of armor stability to this list. Furthermore, Benedicto et al. (2004) experimentally showed the connection between damage progression and the evolution of the wave energy transformation on the slope. Vilchez et al. (2017) experimentally showed that for narrow-banded incident wave trains, the probability density function of the total wave height on a sloping structure evolves from a Rayleigh distribution to a Weibull bi-parametric distribution, depending on the energy dissipation by wave breaking and friction in the porous medium.

These references are among those in consonance with Battjes's proposal, but which are applied to sloping structures that spatiotemporally evolve, depending on wave-structure interaction. The connection between the performance of the three sets of variables (describing the three laws) still hold but now include the dependence on relative water depth, as shown by Moragues et al. (2020) for breaker types, Díaz-Carrasco et al. (2020) for wave energy transformation, and this research for damage progression.

On the other hand, and in line with the major recommendations and technical criteria used throughout the world, the project design of a coastal structure should address the verification of the different failure modes that can affect its stability. Nowadays, this verification is usually performed under the assumption that failure modes are independent. Folgueras et al. (2018) showed the design limitations imposed by this hypothesis. ROM 1.1 (2018) describes a project design methodology based on the progression of damage and concomitant failure modes that could trigger other failure modes. It is also based on the decision regarding when to repair the structure to avoid its collapse. A new challenge for maritime and coastal engineering is to improve the current state of the art and to develop new design tools based on the knowledge of the integrated performance of coastal structures, which would lead to a more integral and unified methodology.

From this perspective, physical experiments on coastal structures should provide a multivariate response. Even though some of them are not functions of the same set of dimensionless factors, all of them are correlated. This research shows the power of the method of Dimensional Analysis (DA) whose validity was established by the Buckingham π-theorem for univariate responses in the early 20th century. Eck et al. (2020) extended the theorem to the multivariate case, and developed basic criteria for the multivariate design of DA.

Nevertheless, to prevent the failure of the DA model, (e.g., the omission of a key explanatory variable), certain precautions should be taken, such as the robust-DA design approach, (Albrecht et al., 2013). Moreover, the statistical analysis of the data should be strengthened by the previous formalization of the DA in the form of regression analysis, latent errors in covariates and robustness (Shen et al., 2014) and the verification of the homogeneity of the data set. Moreover, the statistical invariance principle recognizes that the outcome of a physical experiment should be the same if the measurement scale were transformed.

Thus, the potential relationship between the π-theorem and statistical invariance put the theorem in a stochastic framework to quantify uncertainties in deterministic physical models (Lee and Zidek, 2020).

8. Conclusions

Revetments, dikes, and mound breakwaters are three of the most common coastal and harbor structures because of their ability to break and/or dissipate wave energy, and also because a wide variety of materials and armor unit sizes can be used in their construction. Their hydrodynamic performance and damage evolution depend on the kinematic and dynamic incident wave transformation regimes, which occur when the waves interact with the structure. For many years now, a wide variety of alternatives for the protection, adaptation, and mitigation of the coastline in the face of global warming have been formulated. This challenge necessarily involves quantifying the resilience of structures along with their intrinsic and epistemic uncertainty.

In practical coastal engineering, the design and stability of rock-armored dikes and breakwaters are verified by applying empirical formulas. Currently, most of these stability formulas have the formal structure of the Van der Meer formula.

The objective of this research was to develop a new methodology to assess the damage evolution of sloped coastal structures by applying dimensional analysis (DA) to evaluate its dependence on the experimental design and technique. As an example, this analysis focused on a dike with a two-diameter-thick rock layer over an impermeable core under non-breaking conditions before the waves reached the structure. The adequacy of the derived functional relationship was verified with the same experimental data (rock layer over impermeable dikes under irregular waves) originally used to obtain the Van de Meer stability formula. The main conclusions derived from this research are the following:

(1) The re-analysis of Van der Meer's experimental data reveals that the interplay of m, h/L, and H_I/L is a complex process. The effects of relative water depth and wave steepness on the evolution of damage are concomitant and complementary and should not be analyzed separately.
(2) For each of the four dike slopes tested by Van der Meer (1988), there is a functional relationship between the output (damage) S_d and the input determined by an alternate slope similarity parameter and the number of incident waves N_w. This relationship is specific for each slope, and furthermore depends on the experimental design and technique.
(3) For the shallow-water test series, h/L $\approx$ 0.095, the tested interval by Van der Meer was $[0.10 < H_I/h < 0.20]$. The progression of damage might change significantly for relative shallow water depth and large values of the relative wave height at the toe of the slope.
(4) The sigmoid function is proposed as an alternate prediction method. To capture the damage evolution of both the lower tail (initiation of damage) and upper tail (destruction) of the function, the experimental design and technique must be significantly improved.
(5) Given the current state of knowledge, it is uncertain how stability formulas derived from lab-experiments perform for what may be the design condition. This is a major challenge for maritime engineering

One of the main aims of this study was to stimulate innovative research that would ultimately improve and enhance the knowledge and design of tools for revetments, dikes, and breakwaters. However, to advance further in this direction and extend this new model to permeable core typologies, new tests series are necessary. Evidently, the research presented in this paper does not have sufficient scope to replace Van der Meer type formulas. Nonetheless, one of its evident merits is that it reveals an innovative paradigm for the experimental and technical design of coastal structures, which could be further discussed at the Coastlab, International Coastal Engineering, or Coastal Structures Conferences with a view to coordinating and furthering scientific and technical advancement. Only in this way can the major challenges to modern coastal engineering today be satisfactorily addressed.

CRediT authorship contribution statement

Miguel Á. Losada: Conceptualization, Formal analysis, the study, did the analysis of the data, and prepare the manuscript.

Declaration of competing interest

The authors declare that they have no known competing financial interests or personal relationships that could have appeared to influence the work reported in this paper.

Acknowledgements

The author would like to thank Prof. Baquerizo for her comments on an earlier draft of this text and the careful elaboration of the figures. The author is also grateful to P. Díaz-Carrasco and M.V. Moragues for their help during different stages of this research. This work was partially funded by the Spanish State Research Agency (SRA) under the grant PID2019-107508GB-I00/SRA/10.13039/501100011033. Finally, partial funding was obtained for this research from the emeritus professorship mentoring program of the University of Granada.

List of symbols

A_e	Cross-sectional eroded area
C_p	Permeability coefficient
D*	Armor unit parameter
D_{n50}	Nominal diameter of the main armor layer
D_{nc}	Nominal diameter of the core
e	Layer thickness
f	Functional
g	Gravity acceleration
h	Water depth
H	Wave height
H_I	Incident (significant) wave height
H_s	Significant wave height
I_r	Iribarren number
K_D	Hudson coefficient

K_p	Shape factor of the unit piece
L	Wavelength
N_p	Number of displaced armor units
N_s	Stability Number
N_w	Average number of waves
n_c	Number of layers
n_p	Core porosity
P	Notional Permeability number
S_d	Dimensionless level of damage
T	Wave period
T_m	Average wave period
t	Time
t_0	Time to the origin of time
w_t	Width of section measured
Δ_s	Relative rock density
α	Seawards slope angle
β	Leeward slope angle
β_b	Sea bottom slope
μ_w	Dynamic water viscosity
ρ_w	Water density
ρ_s	Unit piece density
ν	Kinematic viscosity
ξ_m, ξ_z	Surf similarity parameter
χ	Alternative similarity parameter

Appendix Ia. Fit parameters of the straight lines (eq. (10)) for the four slopes

Table A1
Parameters of the straight line for the four slopes 1:2, 1:3, 1:4 and 1:6, $N_w = 1000$ and 3000 waves and relative water depth h/L. R^2 is the linear regression coefficient.

Slope 1:2						
	S_d $Nw = 1000$			S_d $Nw = 3000$		
h/L	A_m	B_m	R^2	A_m	B_m	R^2
0.18306	3.8245	22.698	0.84920	3.9579	24.148	0.85295
0.14706	4.7330	30.153	0.93598	5.7433	36.857	0.93406
0.11490	6.7271	45.999	0.72755	6.4715	44.495	0.71348
0.09716	15.760	110.100	0.95053	12.813	90.073	0.97699
Slope 1:3						
	S_d $Nw = 1000$			S_d $Nw = 3000$		
h/L	A_m	B_m	R^2	A_m	B_m	R^2
0.30949	3.4497	15.930	0.98554	4.4798	20.698	0.94498
0.29342	4.1001	18.853	1	5.2731	24.100	1
0.19491	4.1007	23.166	0.98125	4.2227	24.296	0.99445
0.18397	4.9895	28.353	0.88521	5.2536	30.467	0.99941
0.18173	4.4276	25.518	0.95502	4.9084	28.536	0.97837
0.14652	5.0081	30.973	0.97488	4.441	28.227	0.92096
0.11634	8.4794	55.485	0.98106	8.9923	59.262	0.96935
0.10156	5.8899	40.460	0.97210	5.6138	39.109	0.94567
0.09656	3.8557	27.696	0.44339	4.5784	33.080	0.49069
Slope 1:4						
	S_d $Nw = 1000$			S_d $Nw = 1000$		
h/L	A_m	B_m	R^2	A_m	B_m	R^2
0.28941	4.0277	17.961	0.68625	3.4462	16.022	0.64391
0.22213	2.1461	11.916	1	3.5339	18.627	1
0.19523	2.7083	15.097	0.63272	2.4231	14.096	0.54866
0.14709	3.6958	22.889	0.98258	3.0782	19.903	0.94890
0.11490	4.2362	28.804	0.98655	4.8536	33.170	0.97162
0.10106	4.2575	29.707	0.94323	5.3807	37.586	0.93961
0.09270	4.3532	31.275	0.99970	5.3108	38.335	1
Slope 1:6						
	S_d $Nw = 1000$			S_d $Nw = 3000$		
h/L	A_m	B_m	R^2	A_m	B_m	R^2
0.28132	7.4092	31.185	1	12.105	50.799	1
0.22320	–	–	–	–	–	–
0.18630	2.3128	13.046	0.99959	3.1904	17.682	0.98776
0.14964	3.4407	19.739	0.99566	2.4766	15.267	0.91916
0.11777	3.1186	20.415	0.97297	3.0712	20.493	0.988
0.09600	2.3868	17.590	0.94383	2.2305	16.852	0.93363

Appendix Ib. Fit parameters of the sigmoid function (eq. (12)) for slope 1:3

$$\frac{S_d}{S_{d,max}} = \frac{1}{\left[1 + \left(\frac{log(\chi)}{a_\chi}\right)^{\gamma_\chi}\right]} \qquad \frac{S_{d,0}}{S_{d,max}} \leq \frac{S_d}{S_{d,max}} \leq 1$$

Table A2
Parameters of the sigmoid eq. (12), $N_w = 1000$ and 3000, slope 1:3 and relative water depth, h/L.

Slope 1:3, $N_w = 1000$, $S_{d,0} = 0$, $S_{d,max} = 24$		
Coefficients of the best fit (with 95% confidence bounds)		
h/L	a_χ	γ_χ
0.30306	**−3.980** (−4.048, −3.912)	**27.25** (40.92, 13.58)
0.19491	**−5.004** (−5.053, −4.955)	**25.11** (31.73, 18.5)
0.18263	**−5.166** (−5.275, −5.056)	**28.30** (47.45, 9.141)
0.14652	**−5.693** (−5.723, −5.663)	**44.92** (56.16, 33.67)
0.11634	**−6.253** (−6.275, −6.232)	**69.03** (83.51, 54.54)
0.09934	**−6.441** (−6.554, −6.329)	**43.62** (76.45, 10.78)
Slope 1:3, $N_w = 3000$, $S_{d,0} = 0$, $S_{d,max} = 35$		
Coefficients of the best fit (with 95% confidence bounds)		
h/L	a_χ	γ_χ
0.30306	**−4.017** (−4.076, −3.958)	**31.91** (50.08, 13.73)
0.19491	**−5.074** (−5.092, −5.055)	**31.88** (36.27, 27.49)
0.18397	**−5.225** (−5.239, −5.211)	**34.27** (37.51, 31.03)
0.18173	**−5.206** (−5.360, −5.052)	**30.44** (70.56, 9.69)
0.14652	**−5.702** (−5.792, −5.613)	**33.42** (52.94, 13.89)
0.11634	**−6.309** (−6.333, −6.286)	**106,00** (131.90, 80.03)
0.09934	**−6.476** (−6.597, −6.355)	**45.57** (89.54, 1.59)

References

Ahrens, J.P., McCartney, B.L., 1975. Wave period effect on the stability of rip-rap. In: 3rd Civil Engineering in the Oceans Conference, 2, pp. 1019–1034.

Ahrens, J.P., 1989. Stability of reef breakwaters. J. Waterw. Port, Coast. Ocean Eng. 115 (2), 221–234.

Ahrens, J.P., Seelig, W.N., Ward, D.L., Allsop, W., 1993. Wave runup on and wave reflection from coastal structures. In: Proceedings of Ocean Wave Measurement and Analysis (Waves '93) Conference. ASCE, pp. 489–502.

Albrecht, M.C., Albrecht, T.A., Nachtseim, C.J., Cook, R.C., 2013. Experimental design for engineering dimensional analysis. Technometrics 55 (3), 257–270. https://doi.org/10.11080/00401706.2012.746207.

Baquerizo, A., Losada, M.A., 2008. Human interaction with large scale coastal morphological evolution. An assessment of uncertainty. Coastal Engineering 55, 569–580.

Battjes, J.A., 1974. Surf similarity. In: Proc. 14th International Conference of Coastal Engineering. ASCE, pp. 466–480.

Benedicto, M.I., Ramos, M.V., Losada, M.A., Rodriguez, I., 2004. Expected damage evolution of a mound breakwater during its useful life. In: Proc. 29th International Conference of Coastal Engineering. ASCE, pp. 3605–3614.

Bruun, P., Günbak, A.R., 1977. Stability of sloping structures in relation to $\xi = tan\alpha/H/L_0$ and risk criteria in design. Coastal Engineering 1, 287–322.

Castillo, C., Castillo, E., Fernández-Canteli, A., Molina, R., Gómez, R., 2012. Stochastic model for damage accumulation in rubble-mound breakwaters based on compatibility conditions and the central limit theorem. J. Waterw. Port, Coast. Ocean Eng. 138, 451–463.

Churchill, S.W., Usagi, R., 1972. A general expression for the correlation of rates of transfer and other phenomena. AIChE J. 18, 1221–1128.

Clavero, M., Díaz-Carrasco, P., Losada, M.A., 2020. Bulk wave dissipation in the armor layer of slope rock and cube armored breakwaters. J. Mar. Sci. Eng. 8, 152. https://doi.org/10.3390/jmse8030152.

Díaz-Carrasco, P., Moragues, M., Clavero, M., Losada, M.A., 2020. 2D Water-wave interaction with permeable and impermeable slopes: dimensional analysis and experimental overview. Coastal Engineering 158, 103682.

Eck, D.J., Cook, R.D., Nachtsheim, C.J., Albrecht, T.A., 2020. Multivariate design of experiments for engineering dimensional analysis. Technometrics 62 (1), 6–20. https://doi.org/10.1080/00401706.2019.1585294.

Etemad-Shahidi, A., Bali, M., Van Gent, M.R.A., 2020. On the stability of rock armored rubble mound structures. Coastal Engineering 158, 103655.

Folgueras, P., del Rosal, J., Moragues, M.V., López, J.D., Losada, M.A., 2018. Accumulated damage evolution and investment cost of breakwaters. In: 36th International Conference on Coastal Engineering. ASCE.

Gómez-Martín, M.E., Medina, J.R., 2014. Heterogeneous packing and hydraulic stability of cube and cubipod armour units. J. Waterw. Port, Coast. Ocean Eng. 140, 100–108.

Herrera, M., Gómez-Martin, E., Medina, J.R., 2017. Hydraulic stability of rock armors in breaking wave conditions. Coastal Engineering 127, 55–67.

Hudson, R.Y., 1959. Laboratory investigation of rubble–mound breakwaters. J. Waterw. Port, Coast. Ocean Div. 85 (WW3), 93–121.

Hughes, S.A., 2004. Estimation of wave run-up on smooth, impermeable slopes using the wave momentum flux parameter. Coastal Engineering 51, 1085–1104.

Iribarren, R., Nogales, C., 1949. Protection des Ports. In: XVII International Navigation Congress, Lisbon (1949).

Iribarren, R., 1965. Formule pour le calcul des diques en enrochements naturels ou elements artificiels. In: XXI International Navigation Congress, Stockholm, 1965, Sec. II, Theme 1.

Kobayashi, N., Farhadzadeh, A., Melby, J.A., 2010. Wave overtopping and damage progression of stone armor layer. J. Waterway, Port, Coastal, Ocean Eng. 136 (5), 257–265.

Kobayashi, N., Pietropaolo, J.A., Melby, J.A., 2013. Deformation of reef breakwaters and wave transmission. J. Waterway, Port, Coastal, Ocean Eng. 139 (4), 336–340.

Kroon, A., de Schipper, M.A., van Gelder, Pieter H.A.J.M., Aarninkhof, Stefan G.J., 2020. Ranking uncertainty: wave climate variability versus model uncertainty in probabilistic assessment of coastline change. Coastal Engineering 158, 103673.

Lee, T.Y., Zidek, J.V., 2020. Scientific versus Statistical Modelling: a Unifying Approach. Report. arXiv preprint arXiv:2002.11259. Department of Statistics. University of British Columbia. Submitted to Statistical Science.

Lira-Loarca, A., Cobos, M., Losada, M.A., Baquerizo, A., 2019. Storm characterization and simulation for damage evolution models of maritime structures. Coastal Engineering 156, 103620.

Losada, M.A., Giménez-Curto, L.A., 1979. The joint influence of the wave height and period on the stability of rubble mound breakwaters in relation to Iribarren's number. Coastal Engineering 3, 77–96.

Losada, M.A., Giménez-Curto, L.A., 1981. An approximation to the failure probability of maritime structures under a sea state. Coastal Engineering 5, 147–157.

Losada, M.A., Giménez-Curto, L.A., 1982. Mound breakwaters under oblique wave attack; a working hypothesis. Coastal Engineering 6, 83–92.

Losada, M.A., Desire, J.M., Alejo, L.M., 1986. Stability of blocks as breakwater armor units. Journal of Waterway, Port. Coastal and Ocean Division 112 (11), 2392–2401.

Losada, M.A., Baquerizo, A., Ortega-Sánchez, M., Santiago, J.M., 2009. In: Kim, Young C. (Ed.), Socioeconomic and Environmental Risk in Coastal and Ocean Engineering. Handbook of Coastal and Ocean Engineering. World Scientific, pp. 923–952. Section 8, chapter 33.

Madsen, O.S., Grand, W.D., 1976. Quantitative description of sediment transport by waves. Proc. 15th International Conference on Coastal Engineering 1(15) (64), 1092–1112. https://doi.org/10.9753/icce.v15.64.

Melby, J.A., Kobayashi, N., 1998. Damage progression on breakwaters. In: Proc. 26th International Conference on Coastal Engineering, 2, pp. 1884–1897.

Melby, J.A., Kobayashi, N., 1999. Damage progression and variability on breakwater Trunks. In: Proc. Coastal Structures, Santander, Spain, 1, pp. 309–315.

Melby, J.A., Hughes, S.A., 2004. Armor stability based on wave momentum flux. In: Proceedings of Coastal Structures 2003. American Society of Civil Engineers, Reston, Virginia, pp. 53–65.

Miche, R., 1944. Mouvements ondulatoirs des mers en profondeur constante on decroissant. Annals des Points et Chausses, 1U 2, 25–78.

Moragues, M.V., Clavero, M., Losada, M.A., 2020. Wave breaker types on a smooth and impermeable 1:10 slope. J. Mar. Sci. Eng. 2020 (8), 296. https://doi.org/10.3390/jmse8040296.

Moragues, M.V., Losada, M.A., 2021. Progression of wave breaker types on a plane impermeable slope, depending on experimental design. J. Geophys. Res.: Oceans 126 e2021JCO17211.

PIANC, 2016. Criteria for the selection of breakwater types and their related optimum safety levels.. MarCom. Report no 196. The World Association for Waterborne Transport Infrastructure 196, 1–178.

ROM 0.0, 2002. Description and characterization of project factors of maritime structures., Part I. Puertos del Estado, Madrid (Spain), pp. 1–218. http://www.puertos.es/es-es/BibliotecaV2/ROM%200.0-01%20(EN).pdf.

ROM 1.1, 2018. Recommendations for breakwater construction projects, Articles. Puertos del Estado, Madrid (Spain), pp. 1–229. http://www.puertos.es/es-es/ROM/Paginas/ROM-widispe.aspx.

Shen, W., Davis, T., Lin, D.K.J., Nachtsheim, C.J., 2014. Dimensional analysis and its applications in statistics. J. Qual. Technol. 46 (No. 3), 185–198.

Sonin, A., 2001. The Physical Basis of Dimensional Analysis, second ed. Department of Mechanical Engineering, MIT, Cambridge: Cambridge, MA, USA.

Torum, A., 1998. On the stability of berm breakwaters in shallow and deep water. Coastal Engineering Proceedings 1 (26).

Van der Meer, J.W., 1987. Stability of breakwater armour layers-Design Formulae. Coastal Engineering 11 (3), 219–239.

Van der Meer, J.W., 1988. Rock slopes and gravel beaches under wave attack (Ph.D. Thesis). Delft University of Technology 1–144. http://resolver.tudelft.nl/uuid:67e5692c-0905-4ddd-8487-37fdda9af6b4.

Van Gelder, P.A.J.H.M., 2000. Statistical Methods for the Risk-Based Design of Civil Structures (Ph.D. thesis). Delft University of Technology.

Vidal, C., Medina, R., Lomónaco, P., 2006. Wave height parameter for damage description of rubble-mound breakwaters. Coastal Engineering 53, 711–722.

Vílchez, M., Clavero, M., Losada, M.A., 2016. Hydraulic performance of different non-overtopped breakwater types under 2D wave attack. Coastal Engineering 107, 34–52.

Vilchez, M., Clavero, M., Baquerizo, A., Losada, M.A., 2017. An approximation to the statistical characteristics of wind waves in front and from the toe of the structure to the toe of the crown of nonovertopped breakwaters. Coast Eng. J. 59 (No. 3), 1750012.